Alignment and use of the optical test for the 8.4 m off-axis primary mirrors of the Giant Magellan Telescope

S.C. West*[a], J.H. Burge[b], B. Cuerden[a], W. Davison[a], J. Hagen[a], H.M. Martin[a], M.T. Tuell[a], C. Zhao[b], and T. Zobrist[b]

[a]Steward Observatory, University of Arizona, Tucson, AZ 85721, USA;
[b]College of Optical Sciences, University of Arizona, Tucson, AZ 85721, USA
*scwest@email.arizona.edu

ABSTRACT

The Giant Magellan Telescope has a 25 meter f/0.7 near-parabolic primary mirror constructed from seven 8.4 meter diameter segments. Several aspects of the interferometric optical test used to guide polishing of the six off-axis segments go beyond the demonstrated state of the art in optical testing. The null corrector is created from two obliquely-illuminated spherical mirrors combined with a computer-generated hologram (the measurement hologram). The larger mirror is 3.75 m in diameter and is supported at the top of a test tower, 23.5 m above the GMT segment. Its size rules out a direct validation of the wavefront produced by the null corrector. We can, however, use a reference hologram placed at an intermediate focus between the two spherical mirrors to measure the wavefront produced by the measurement hologram and the first mirror. This reference hologram is aligned to match the wavefront and thereby becomes the alignment reference for the rest of the system. The position and orientation of the reference hologram, the 3.75 m mirror and the GMT segment are measured with a dedicated laser tracker, leading to an alignment accuracy of about 100 microns over the 24 m dimensions of the test. In addition to the interferometer that measures the GMT segment, a separate interferometer at the center of curvature of the 3.75 m sphere monitors its figure simultaneously with the GMT measurement, allowing active correction and compensation for residual errors. We describe the details of the design, alignment, and use of this unique off-axis optical test.

Keywords: telescopes, optical alignment, aspheres, null lens, interferometry, optical testing

1. INTRODUCTION

The Giant Magellan Telescope (GMT) consists of a 25m f/0.7 near-parboloid composed of an array of seven 8.4m segments.[1]-[3] The principal optical test for the six off-axis segments has been described previously.[4]-[6] Since the last paper was written in 2008, the test has been operational and in use guiding the polishing of the first GMT off-axis segment. This paper presents on update of its status and a summary of the practical aspects of aligning and using the test.

Null lens systems for large axisymmetric mirrors are placed into relatively small canisters where the alignments of the optical elements are precisely controlled and remain stable until the mirror is finished.[7],[8] Verifying the null lens is relatively straightforward by rotating the null lens to map non-axisymmetric errors and using certification holograms.[9] In contrast, the null lens for the off-axis GMT segments must maintain precise absolute alignment over a 32m path length. Power must be controlled to match the radius of curvature of all the segments. Tilts of large optical elements are used to set the absolute correction of low order errors such as astigmatism and coma. Rotation of the null corrector over the test optic is impossible, and there is no place in the test beam where a certification hologram can work.

Section 2 provides a brief review of the test illustrating the optical components and wavefront shaping of the optical beam. Section 3 describes the error budget for the test and the allowable tolerances. Section 4 describes the large fold sphere (hereafter LFS), its supports, and figure optimization. Section 5 describes the package of smaller optical elements known as Sam which contains the small fold sphere (hereafter SFS), the measurement hologram, and the reference hologram. Section 6 presents the concepts, procedures, and results of aligning and using the test.

2. TEST DESCRIPTION

Figure 1 illustrates the ray diagram for the test. The segment aperture is drawn onto the parent. The null corrector consists of 2 fold spheres and a transmission hologram. Most of the wavefront shaping is done with the two tilted spheres. Table 1 shows that each sphere shapes large amounts of power, astigmatism, and coma reducing the P-V surface error from 14.2mm at the segment to 320µm. Remaining aberrations including high-order aspheric departures are corrected with the transmission hologram. The reference hologram is a removable alignment aid as described later.
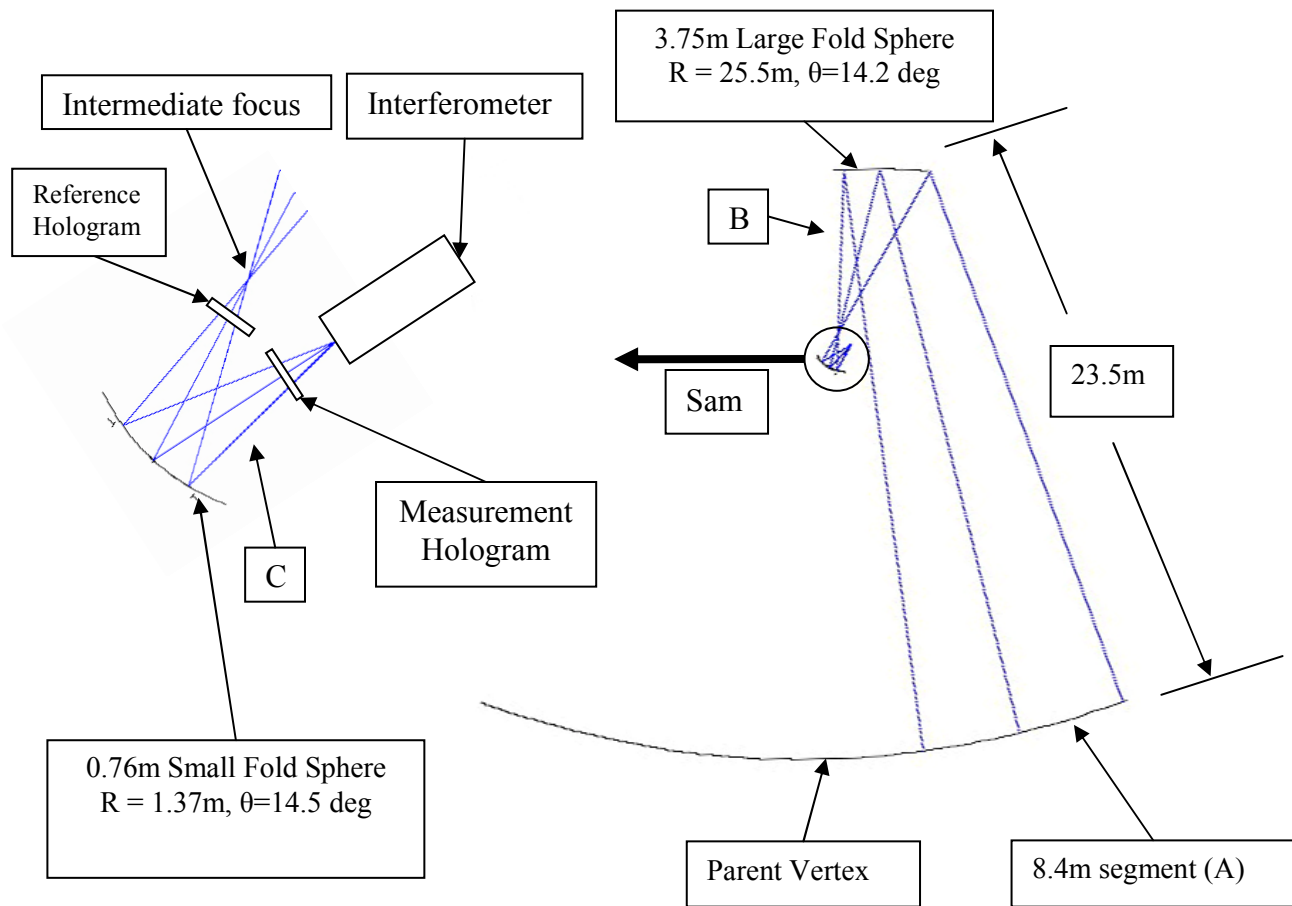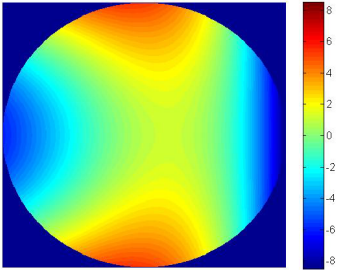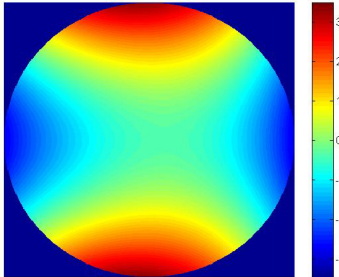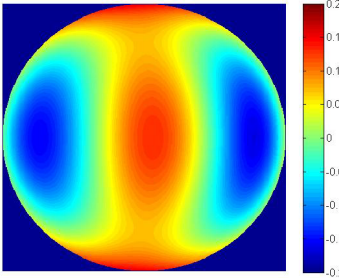

Figure 1: Ray diagram of the principal optical test for a GMT off-axis segment (right) and a close-up of Sam (left). The segment is shown placed on the 25m f/0.7 parent mirror. The null corrector consists of two fold spheres and a transmission hologram. θ is the angle of incidence of the ray that goes to the center of the GMT segment. 'A', 'B', and 'C' refer to beam locations where wavefront maps are shown in **Table 1**.

Table 1: Low order Zernike surface amplitude fit coefficients and total P-V (mm) surface are shown vs. location in principal test beam. The parent vertex (and +y) point to the left. The Zernike polymomials are normalized to 1 at the edge of the aperture.

Beam location	A0	CY	P-V All modes
A: At segment	6.40	1.58	14.2
B: Just after large fold sphere	3.18	0.25	6.1
C: Between small fold sphere and hologram	0.15	0.02	0.32

3. ALIGNMENT ERROR BUDGET

The alignment of the GMT optical test has three categories: 1) alignment of the Sam components with respect to one another to 10-20 µm, 2) 50-100 µm alignment of the large fold sphere and GMT segment with respect to Sam, and the stability of the alignment throughout the testing period. The effects of misalignment have been determined through direct simulation in Zemax. A given component is misaligned, any effects this misalignment has on other optical

components are simulated, and then the error they produce on the segment is estimated. However, the segment error produced by the test misalignment is relaxed because in actual operation of the telescope, each segment's performance is optimized by: 1) a small radial (off-axis) displacement, 2) clocking compensation (rotation about the center of the segment), and 3) bending of the segment with the active supports. The corrections are determined by analysis as the combination of alignment and bending that minimizes bending force and residual segment surface error. Active optics compensation and the optical specifications of the segment are described elsewhere. [4]-[6],[10]

The resulting top-level alignment error budget is shown in Table 2. Although this budget has been shown previously[6], several quantities have since been updated.

Table 2: Effects of misalignment of the optical components of the GMT principal optical test on the off-axis distance, clocking angle, correction force, and residual surface error of the GMT segment. Parameters are local to each component with the z-axis perpendicular to the surface of the component.

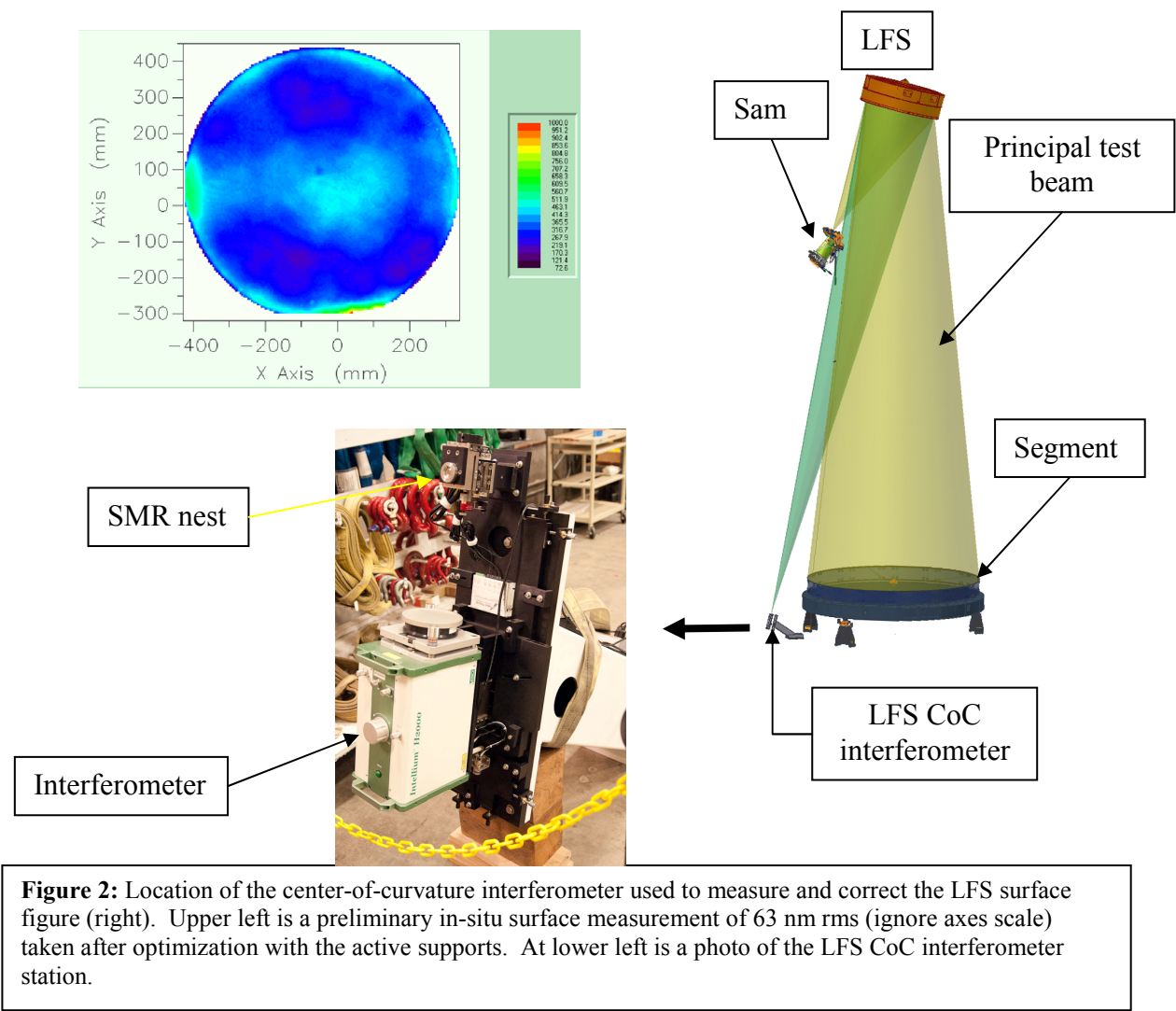| Element	Parameter	Uncertainty (μm, μrad)	Effect on the GMT mirror segment			
			radial shift (mm)	clocking (arcsec)	correction force (N rms)	residual rms surface (nm)
interferometer	x	2	0.0	0	0.2	0.2
	y	2	0.0	0	0.6	0.6
	z	11	0.1	0	2.3	2.7
LFS	x	22	0.0	0	1.4	1.5
	y	22	0.0	0	4.6	5.2
	z	13	0.0	0	2.0	1.8
	R	20	0.0	0	0.4	0.4
	0° astig	50 nm rms	0.0	0	1.0	1.0
	45° astig	50 nm rms	0.0	0	0.7	0.5
reference hologram	X	61	0.0	0	0.3	0.5
	Y	62	0.0	0	1.2	1.5
	Z	61	0.6	0	3.5	4.9
	θ_x	26	0.1	0	5.4	5.3
	θ_y	29	0.0	1	2.1	2.2
	θ_z	43	0.0	1	1.2	1.2
SFS	z	73	0.8	0	6.0	8.0
	θ_x	7.7	0.4	0	3.0	3.0
	θ_y	7.7	0.0	4	0.9	0.9
	R	200	0.3	0	1.3	1.9
	0° astig	100 nm rms	0.0	0	1.6	2.1
	45° astig	100 nm rms	0.0	3	1.1	1.3
GMT segment	z	120	0.2	0	2.7	3.2
Components of Sam not measured with reference hologram			0.2	3	7.1	7.4
Sum in quadrature			1.2	6.6	13.9	15.8
Alignment error budget allocation			2	50	42	structure function

The change in this table from the previous version allows for increased errors in determining the orientation of the reference hologram. The loosened tolerances still fit comfortably within the segment's error budget. 'R' is radius of curvature, and the astigmatism is expressed as rms surface error. The residual segment surface error is due to imperfect

bending, because a finite number of bending modes are combined for the correction. Using more modes produces a better surface error but increases the maximum bending force. This Table should not be considered final because recent work has identified several small effects that are not yet completely analyzed.

4. LARGE FOLD SPHERE

The large fold sphere (LFS) shapes over half of the astigmatism and most of the coma of the null test. It is 3.75m in diameter with a radius of curvature near 25.5m. The honeycomb mirror was cast from Ohara E6 borosilicate, generated, and polished at the University of Arizona Steward Observatory Mirror Laboratory (SOML).

The LFS is allocated 20% of the structure function error budget for polishing the segment. This roughly translates to a surface figure error of 28 nm rms. This does not include astigmatism which is treated separately as shown in Table 2. Errors in excess of the structure function budget must be subtracted from the measured figure of the GMT segment. In order to achieve the best surface, the mirror shape can be optimized with active supports using feedback from a center of curvature interferometer. Preliminary figure optimizations typically achieve 60 nm rms surface. This measurement system is incorporated into the optical test (Figure 2).

Figure 2: Location of the center-of-curvature interferometer used to measure and correct the LFS surface figure (right). Upper left is a preliminary in-situ surface measurement of 63 nm rms (ignore axes scale) taken after optimization with the active supports. At lower left is a photo of the LFS CoC interferometer station.

The mirror is supported by 20 single and 19 two-axis actuators (Figure 3). Each of the axial actuators has a remotely adjustable force for mirror figure correction. The mirror position in the cell is set by six struts that connect the mirror

backplate to the cell (not shown in Figure 3). Each strut has an in-line load cell that (taken in combination) is used to measure the reaction forces and moments on the mirror. The force of the diagonal axis of the two-axis actuators is also remotely adjustable, and combined with the axial actuators is used to remove global forces and moments on the mirror. The cross-lateral force is removed by clocking the cell. The actuator force resolution is 0.25 N.

Alignment of the LFS uses a hexapod that attaches the cell weldment to the test tower (Figure 4). The hexapod struts have a resolution of 1.25 μm and a 17 μm lost motion error upon reversing direction, so target positions are approached from the same direction.
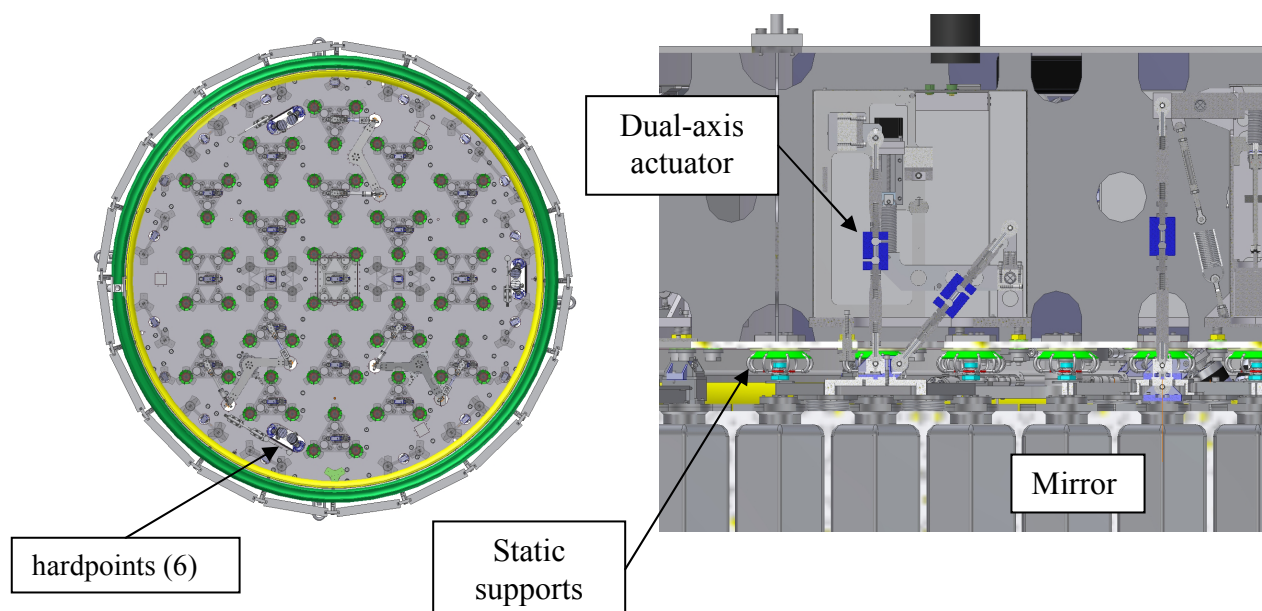

Figure 3: Top view (left) of the LFS load spreader distribution and six hardpoints. Cutaway (right) of the LFS support system showing both a dual- and single-axis active actuator and static supports.
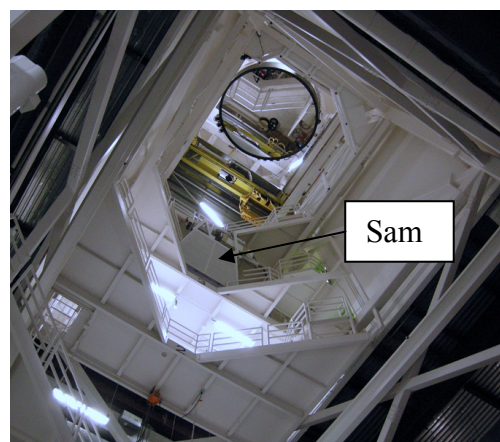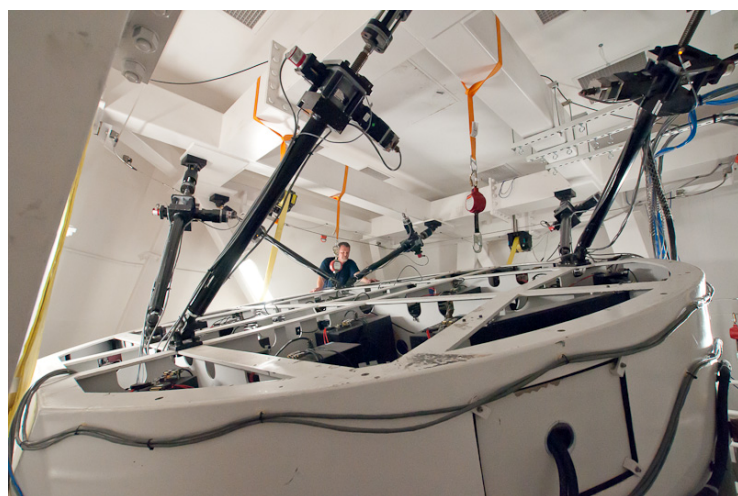

Figure 4: View of the LFS positioning hexapod which connects the LFS weldment to the top of the test tower (left). View of 3.75m LFS and Sam from the segment (right).

5. SAM

Sam contains the small fold sphere (SFS), its support and positioning systems, the transmission measurement hologram, the reflection reference hologram, null test interferometer, and alignment aids (Figure 5). The interferometer is a 4D Technology High Power Phasecam with a diverger used at f/1.9. The output beam reflects off a steering flat and into the measurement hologram. The measurement hologram is contained in an invar frame called the Cradle that is kinematically connected to the Sam frame which itself is kinematically attached to the test tower (not shown). The beam continues through the hologram onto the SFS and reflects to the LFS. A reflection reference hologram can be moved into and out of the Sam beam. This hologram provides a null test for Sam, and allows the user to transfer the orientation of the Sam wavefront to the alignment of the LFS and segment. This will be detailed in Section 6 with the other alignment aids shown in Figure 5.
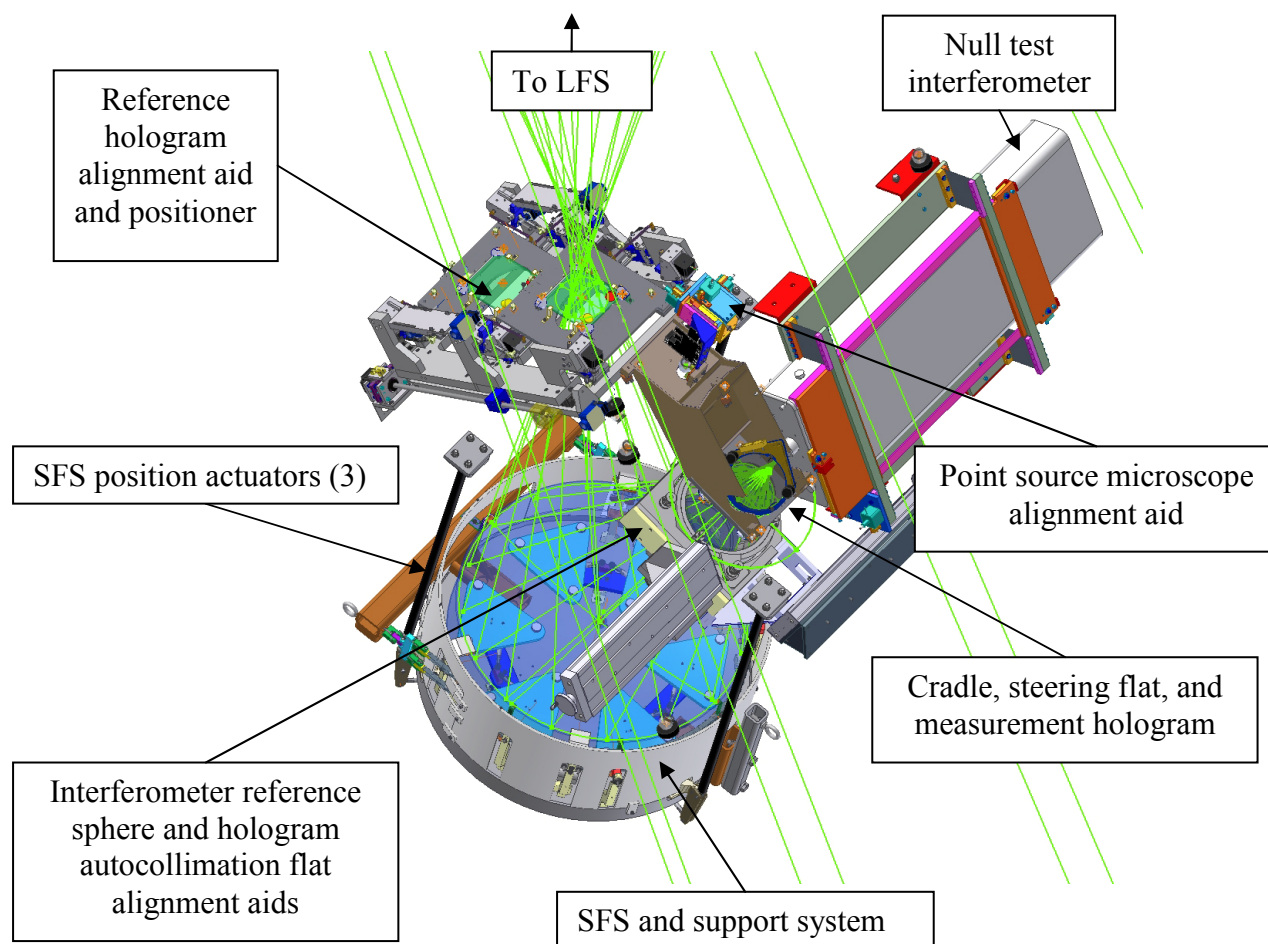
Figure 5: Identification of the components of Sam. See text for details.

The SFS is a 0.76m diameter made from Zerodur. The SFS shapes about one half of the astigmatism and a small amount of coma in the null test. The sphere surface is allocated 10% of the segment polishing wavefront budget or about 14 nm rms. Residual astigmatism in the surface is treated separately as shown in Table 2. The mirror was polished at the University of Arizona College of Optical Sciences using their robotic swing-arm machine to a surface accuracy of 4 nm rms. A photo of Sam in the test tower and the final polished surface figure map is shown in Figure 6.

In Sam, the SFS is supported passively on an 18-point whiffle tree and contains no active figure correction. Lateral support is provided by a belly-band chain mount, and three tangent arms provide radial and clocking constraints. When mounted in the Sam cell, the SFS has a surface figure of 15 nm rms including residual astigmatism, the latter of which is treated separately in the error budget as shown in Table 2. The SFS cell is connected to the Sam frame with three positioning actuators capable of adjusting the SFS pointing to one μrad.
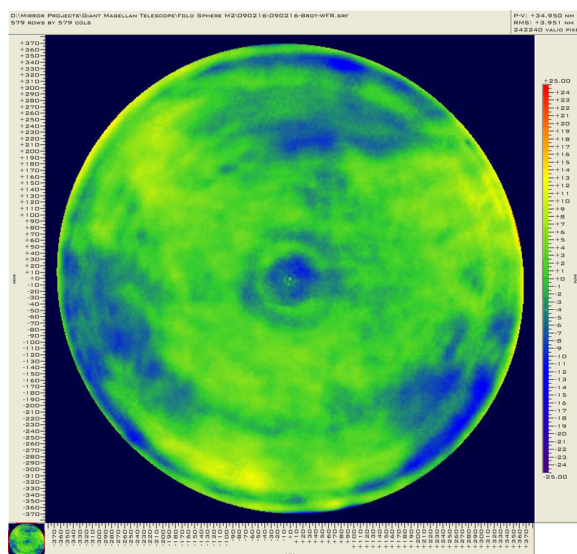

Figure 6: The small fold sphere attached to the test tower is shown at right. The final polishing surface map (left) is 4 nm rms, and this increases to 15 nm rms when mounted in the Sam support cell.

6. ALIGNMENT CONCEPTS AND PROCEDURES

The alignment of the test consists of aligning Sam to high precision, and then using knowledge of the position and orientation of its wavefront to align the LFS and segment.

6.1 Alignment of Sam

The alignment of Sam consists of positioning the interferometer to the measurement hologram, verifying the SFS radius of curvature, and aligning the SFS to the measurement hologram. Refer to Figure 5 for Sam component identifications.

The measurement hologram (shown in Figure 7) has alignment aids that allow both the interferometer and the SFS to be registered to it. The measurement hologram actually consists of 3 holograms: 1) the main transmission hologram that nulls the remaining wavefront error in the null test, 2) a spherical reflection hologram annulus that allows the tilt errors of the interferometer to be seen, and 3) a transmission hologram that supports an autocollimation test used with a flat mirror that measures focus error in the interferometer position. Additionally, the hologram substrate has 4 bullseyes placed in the corners that are used to identify the center and clocking orientation of the measurement hologram. The corner mounts each contain an SMR (spherically mounted retro-reflector) nest for the laser tracker and a ball to engage the kinematic mount on the Cradle. Both optical and mechanical CMMs (coordinate measuring machines) are used to register the SMR positions to the center of the main hologram. The optical CMM measures the bullseyes and the xy

positions of the SMRs. The mechanical CMM verifies these positions and measures the z-height of the SMRs from the substrate surface. Also shown are tilt fringes from the intentionally mis-aligned interferometer.
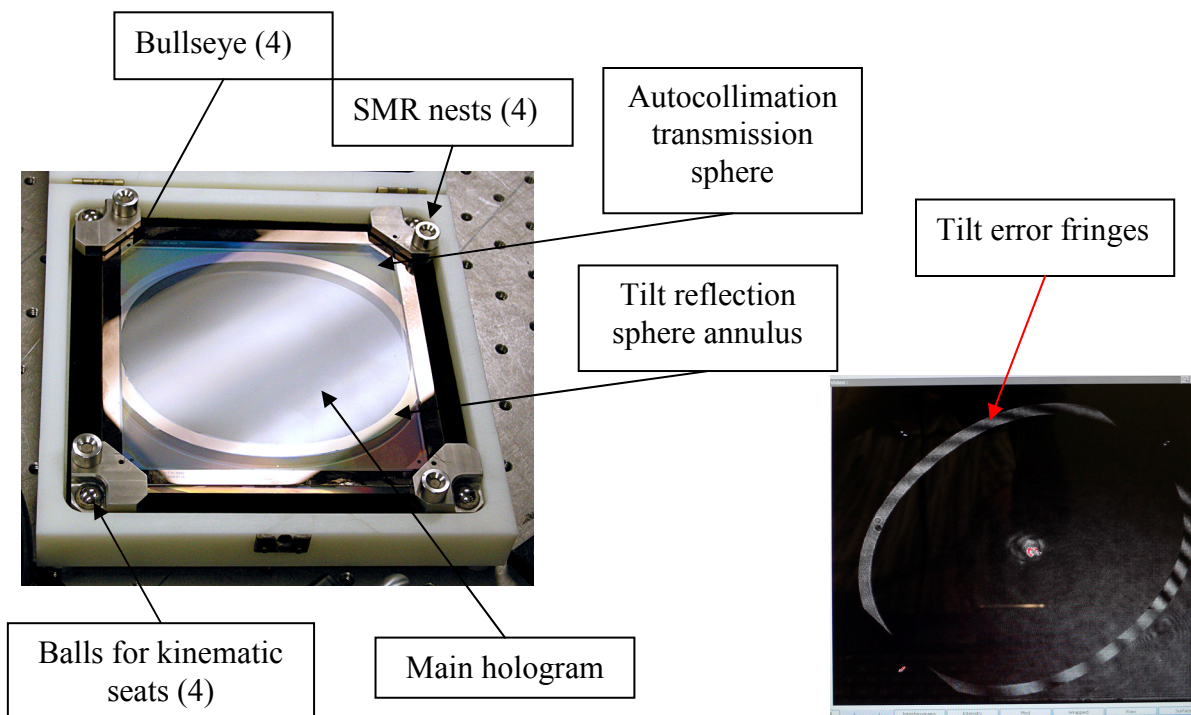

Figure 7: The measurement hologram is shown at left, and an interferogram of the tilt annulus hologram (right) was taken with an intentionally misaligned interferometer. See text for details.

The invar cradle (Figure 8) contains the kinematic mounts for the measurement hologram and an SMR nest for the position of the SFS center-of-curvature point. The kinematic mount consists of the usual cone and slot arrangement, but instead of a third point with a flat surface, a flexure teeter-totter contains two flats and gives support for the other 2 corners of the hologram. Each kinematic attachment contains a magnet to hold the hologram against gravity. Testing was done to insure that the flexure teeter-totter and magnets did not over constrain the kinematic mount or distort the hologram substrate, yet insure that the hologram would be held in place against gravity. The optical design program provides the location of the SFS CoC position relative to the hologram center. A laser tracker is used to adjust the position of a tracker SMR relative to the hologram. This position is verified with the mechanical CMM to insure compliance with the error budget of Table 2 (10 μm xyz or 7.7 μrads error of the SFS x and y angles).

Now that the SFS CoC point is positioned relative the measurement hologram, Figure 9 illustrates how the Point Source microscope (PSM) is used to align the SFS to the CoC ball in the Cradle. The PSM (Optical Perspectives Group, Tucson AZ) is an autocollimator and source with a detector for centroiding the return beam. A 20x microscope objective diverger is attached to the output. The PSM is mounted to a remotely controlled positioner, and is aligned to center the return beam that reflects from the surface of the CoC ball. When the CoC ball is removed, the PSM fills the SFS, and the SFS positioners are adjusted to align the SFS position and orientation to the CoC ball center using the detector of the PSM. The SFS radius of curvature has been previously measured by using a laser tracker to measure the distance between the CoC ball and an SMR contacting the SFS surface in several locations.
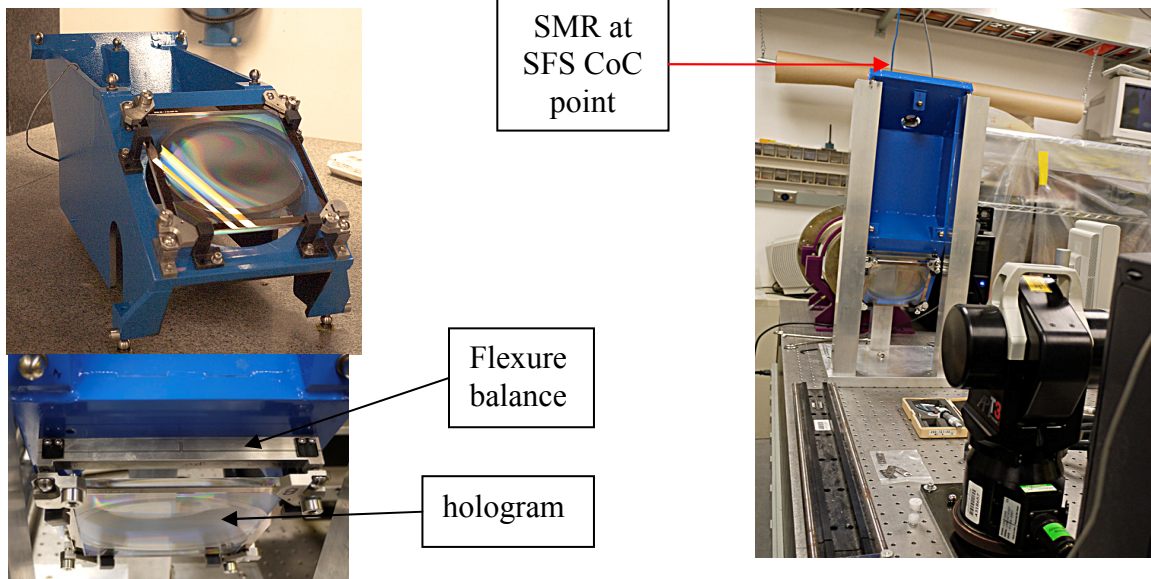
Figure 8: The invar Cradle with the measurement hologram attached (upper left). At right is the adjustment of the SFS CoC position with a laser tracker relative to the measurement hologram. The position is verified with a mechanical CMM prior to installing into Sam. After installation, the position is again verified. A flexure balance with two flats allows the hologram to be supported at 4 points (lower left).
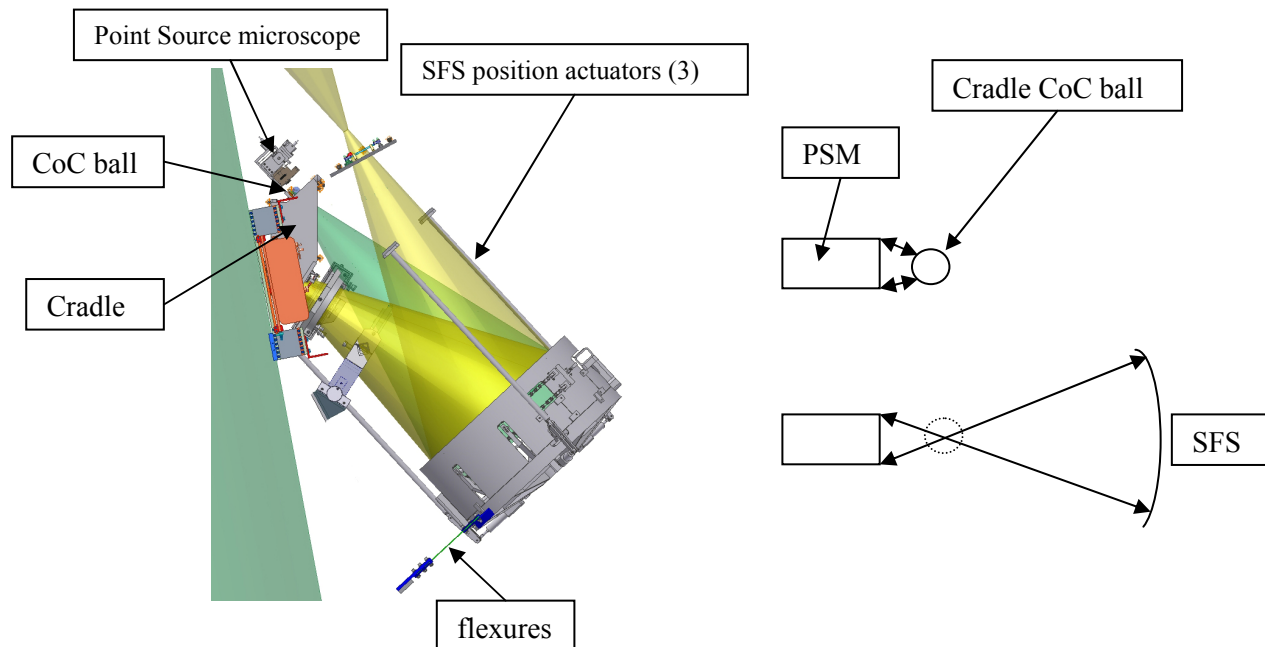

Figure 9: Use of the Point Source microscope (PSM) to adjust the position and orientation of the SFS is shown in a side view of Sam (left). The PSM is aligned to the SFS CoC ball in the Cradle (upper right). The ball is removed, and the SFS position actuators are adjusted to bring the SFS radius of curvature point to the ball center (lower right).

6.2 Determining the position and orientation of the Sam wavefront

In order to align the LFS and segment to the Sam wavefront, a special reflection reference hologram is inserted into the Sam beam near the intermediate focus (its position in Sam is shown in Figure 5 and as the unlabeled hologram in Figure 9). The hologram contains a reflective pattern that matches Sam's wavefront and sends a null wavefront back to the interferometer. It is attached to a six DOF positioner that is also capable of moving the hologram in and out of the Sam beam. The hologram is inserted into the Sam beam, and its position is refined until the interferometer fringes are nulled. Now the hologram substrate defines the position and orientation of the Sam beam.

The hologram contains alignment aids that allow the test tower laser tracker to measure its position and orientation which are then used to align the LFS and the segment to the Sam wavefront. Like the measurement hologram, the reference hologram has corner pieces that fit to a kinematic mount on the positioner and contain SMR nests. However, measuring these SMRs with the laser tracker provides insufficient accuracy to define the orientation of the reference hologram (typically 30-40 µrad which itself is larger than the total allocation given to the reference hologram shown in Table 2). Instead, the angles are determined by viewing SMRs mounted to the test tower structure in reflection from mirrors that are mounted to the hologram substrate (Figure 10). The orientation of the hologram is computed from the laser tracker reflected positions of the SMRs, the actual positions of the SMRs, and knowledge of the plane mirrors' relationship to the hologram center.[11]
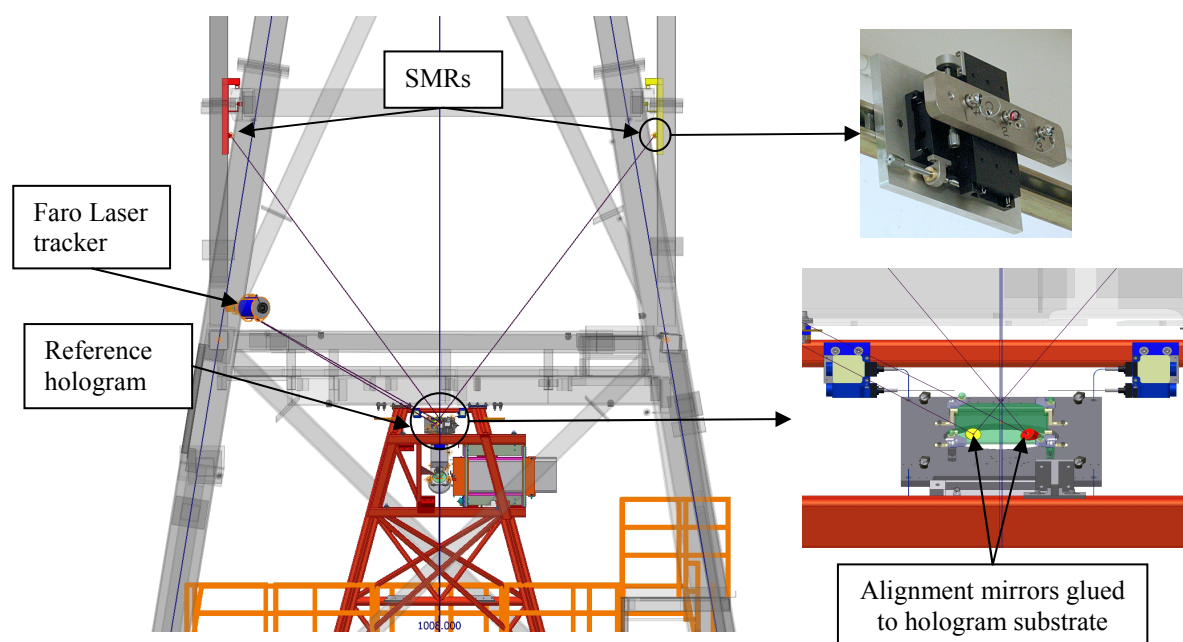

Figure 10: The accuracy of determining the reference hologram orientation is increased by viewing SMRs mounted to the tower structure (left) in reflection from plane mirrors mounted on the hologram substrate (lower right). The reflection SMR is pointed at the plane mirror on the hologram, and it is flanked by 2 SMRs pointed at the laser tracker (upper right). Using the positions of the two outer SMRs, the position of the reflection SMR is known.

Using reflected SMR positions to determine the orientation of the reference hologram requires mounting plane mirrors to the hologram substrate that have a known absolute angular relationship to the hologram. The reference hologram and the setup for aligning the plane mirrors are shown in Figure 11. Two pairs of gratings are manufactured onto the hologram substrate. Each pair has a known azimuth and altitude offset from the y-axis and hologram plane respectively. Duplication was considered a good cross check. A PSM autocollimator (without the microscope objective) is used to measure the angle differences between the gratings and the plane mirrors. A Zerodur reference window is oriented perpendicular to the grating angle. The PSM beam is moved onto each optic with an xy stage. Measurements of the

mirrors and gratings are always made relative to the beam returned by the reference window which is held constant throughout the measurements.
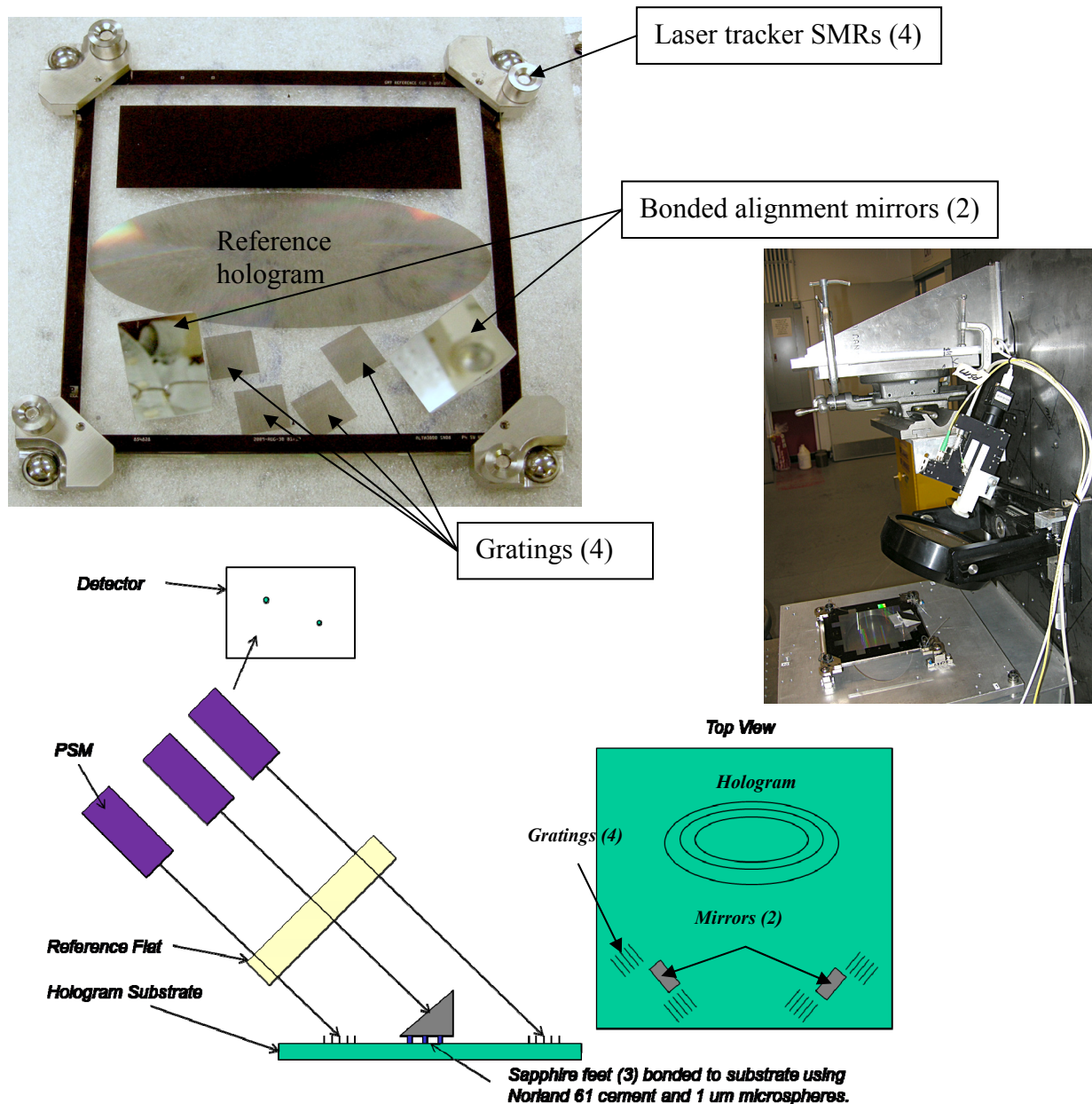

Figure 11: The reference hologram and its alignment aids (top). The method of registering the alignment mirrors to the hologram plane (bottom) is explained in the text. Right center is the setup to register the plane mirrors to the gratings.

The flat mirrors are bonded to the hologram substrate with three sapphire disks which are lapped to make the mirrors match the gratings to 15 µrad. The PSM then measures the offset between the gratings and mirrors to an accuracy of 8 µrad.

We note that initially, the reference hologram was mounted kinematically to a plate which contained the alignment mirrors. However, the kinematic mount was repeatedly compromised by contamination causing the absolute alignment between the hologram and mirrors to be lost. Therefore, it was decided to bond the mirrors to the substrate directly.

Once bonded, the orientation of the plane mirrors is known relative to the gratings. However, any substrate distortion must be included in the angular offsets. The substrate is measured with a large beam WYKO interferometer. Local tilt differences between the substrate at the center of the hologram and the substrate at the grating positions are included in the angle offsets of the plane mirrors (Figure 12). Also shown in a typical nulled interferogram from the reference hologram in the Sam beam.
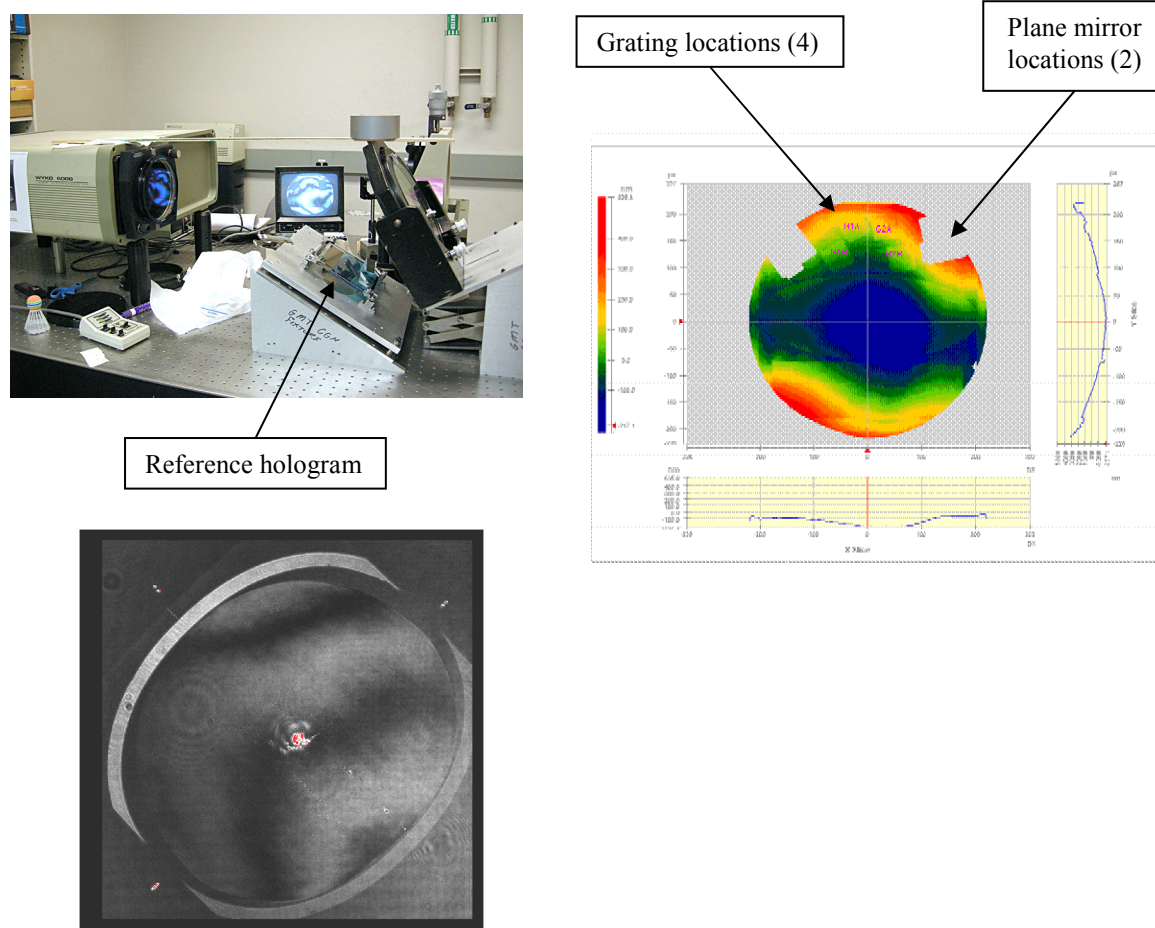

Reference hologram

Grating locations (4)

Plane mirror locations (2)

Figure 12: Hologram substrate distortion was measured with a WYKO interferometer and the hologram supported in the same orientation as it has in Sam (upper left). The phase map was used to find the tilt offsets between the center of the hologram and the gratings to which the plane mirrors are registered (upper right). The offsets are between 5 and 8 µrads, and are included in the laser tracker measurements to determine the orientation of the Sam beam. A typical interferogram of the reference hologram in its nulling orientation in the Sam beam (lower).

6.3 Aligning the LFS and segment to the Sam wavefront

The previous two sections describe how Sam is aligned and a method for determining the position and orientation of the Sam wavefront. The laser tracker can now record the orientation of the Sam wavefront and use it to guide the alignment of the LFS and segment. Figure 13 shows the entire set of 16 laser tracker SMRs used in aligning the principal test. The 4 SMRs attached to the measurement hologram are not shown, because they are used to set the position of the SFS center of curvature point once.

The optical design program gives the alignment targets relative to the reference hologram position and orientation. These values are constant unless something fundamental changes (e.g., LFS radius of curvature is refined). Both the segment and the LFS each have 4 SMRs attached to the outer edge of the mirror surfaces. The LFS alignment uses either

these four SMRs or the LFS CoC SMR. The LFS SMRs need only be contacted to the edge of the optic without knowing their absolute coordinates with respect to the mirror vertex or azimuth since the optic is spherical. The segment edge SMRs are used to position, piston, and clock the optic into the proper location. Their positions are recorded relative to the segment center in x, y, z, and clocking angle relative to the line between the segment and parent centers.
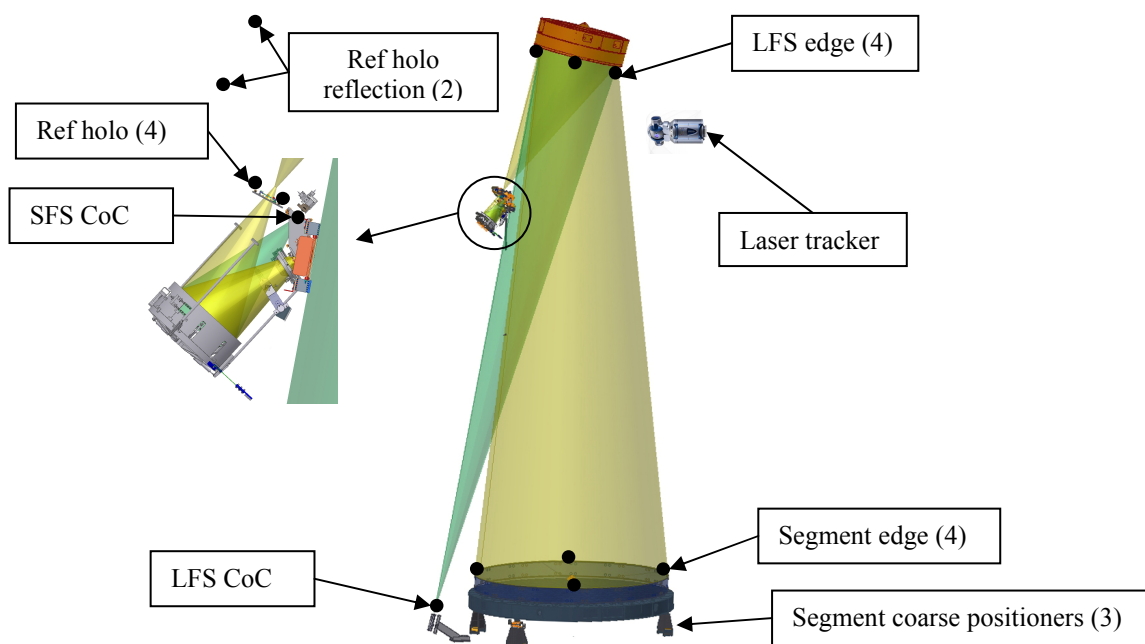

Figure 13: Diagram showing the locations of the 16 laser tracker SMRs used in the active alignment of the GMT principal test.

A MATLAB program reads the laser tracker data for the reference hologram and provides the alignment information for the LFS and segment positioners. Although there is an alignment viewing screen at the focus of the interferometer diverger, the alignment from the MATLAB program is all that is routinely required. The laser tracker is controlled and read from the main control computer using the Faro Java API (application programming interface) making the data available to the support programs written in house.

The segment is mounted on a six-axis positioner with a resolution of 20 µm (shown in Figure 13 and in close-up in Figure 14) which is sufficient for segment translation and clocking. Once it and the LFS center of curvature are aligned, the reference hologram is removed from the Sam beam. The remaining degrees of freedom are tip and tilt of the segment. A fine-positioner is built into the hydraulic supports of the segment in order to adjust tip and tilt with sub-micron resolution and is used to null the fringes for the interferometric test.

If necessary, the segment may be moved from its nominal position to obtain a better match to the test wavefront, but any move must be a fraction of the tolerances shown in Table 2 (2mm off-axis distance and 50-arcseconds clocking).
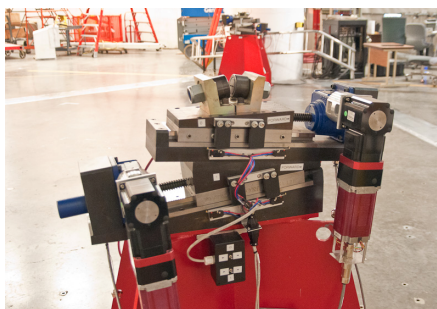
Figure 14: A close-up view of one of three segment coarse positioners consisting of a pair of tilted slides.

7. SUMMARY

The components and alignment of the GMT principal test for the first off-axis segment have been described. The test consists of a non-axisymmetric null lens system that is over 30m long and precisely aligned. The wavefront shaping is performed by 2 tilted spheres and a hologram. The interferometer, small fold sphere, and measurement hologram are combined into a unit called Sam. The position and orientation of the Sam wavefront are determined with a null test created by a second hologram. Alignment aids manufactured into this hologram allow the large fold sphere and GMT segment to be aligned to the Sam wavefront. As of this writing, the test has been used to guide segment polishing for six months, and is very close to realizing the final accuracy specifications given in the top-level error budget.

Future work will concentrate on removing LFS surface figure errors from the test and refining the alignment of the reference hologram to the Sam wavefront. Complete automation of the alignment will help improve efficiency for this and the following GMT segments.

ACKNOWLEDGEMENT

REFERENCES

[1] M. Johns, "Progress on the GMT", Proc. SPIE 7012, 70121B (2208).
[2] M. Johns, "The Giant Magellan Telescope", Proc. SPIE 6267, 626729 (2006).
[3] H.M. Martin, J.R.P. Angel, J.H. Burge, B. Cuerden, W.B. Davison, M. Johns, J.S. Kingsley, L.B. Kot, R.D. Lutz, S.M. Miller, S.A. Shectman, P.A. Strittmatter, and C. Zhao, "Design and manufacture of 8.4m primary mirror segments and supports for the GMT." Proc SPIE 6273, 62730E (2006).
[4] H.M Martin, R. G. Allen, J.H. Burge, D.W. Kim, J.S. Kingsley, M. Tuell, S.C. West, C. Zhao, and T. Zobrist, "Fabrication and testing of the first 8.4m off-axis segment for the Giant Magellan Telescope," Proc. SPIE 7739 (2010).
[5] J.H. Burge, L.B. Kot, H.M. Martin, R. Zehender, and C. Zhao, "Design and analysis for interferometric measurement of the GMT primary mirror," Proc. SPIE 6273, 62732T (2008).
[6] J.H. Burge, W. Davison, H.M. Martin, and C. Zhao, "Development of surface metrology for the Giant Magellan Telescope primary mirror," Proc. SPIE 7018, 701814 (2008).
[7] J.H. Burge, L.R. Dettmann, and S.C. West, "Null correctors for 6.5-m f/1.25 paraboloidal mirrors," in Fabrication and Testing of Aspheres (FTA), OSA Trends in Optics and Photonics, (1999).
[8] J.H. Burge, D. Anderson, D.A. Ketelsen, and S.C. West, "Null test optics for the MMT and Magellan 6.5 m f/1.25 primary mirrors," Proc. SPIE 2199, 658 (1994).
[9] J.H. Burge, "Certification of null correctors for primary mirrors," Proc. SPIE 1994, 248 (1994).
[10] H.M. Martin, J.H. Burge, B. Cuerden, W.B. Davison, J.S. Kingsley, W.C. Kittrell, R.D. Lutz, S.M. Miller, C. Zhao, and T. Zobrist, "Progress in manufacturing the first 8.4m off-axis segment for the Giant Magellan Telescope," Proc. SPIE 7018, 70180C (2008).
[11] J.H. Burge, P. Su, C. Zhao, and T. Zobrist, "Use of a commercial laser tracker for optical alignment," Proc. SPIE 6676, 66760E (2007).